

Two-compartment pharmacokinetic modeling of targeted molecular MRI contrast agents

M. Oostendorp^{1,2}, K. Douma^{1,2}, T. M. Hackeng^{1,2}, M. A. van Zandvoort^{1,2}, M. J. Post^{1,2}, and W. H. Backes^{1,2}

¹Maastricht University Medical Centre, Maastricht, Netherlands, ²CARIM, Maastricht, Netherlands

Introduction

Molecular MRI allows the specific detection of biomolecules that are upregulated during disease. To this extent, contrast agents (CAs) are used that home to the targeted biomolecules via high affinity ligands coupled to the CA. Activated endothelial cells in tumor angiogenesis provide well suited disease markers, which are easily accessible for circulating CAs. Several studies have already demonstrated the MRI responses induced by these targeted particles in terms of increases in signal intensity^{1,2} or relaxation rates³. However, the dynamic homing behavior and pharmacokinetics of targeted CA particles are largely unknown. Moreover, the intrinsic low molecular sensitivity of MRI requires the use of relatively large CAs, which may poorly penetrate deep tumor tissue. The goal of this work was to develop a pharmacokinetic model to describe the dynamic behavior of the previously developed cNGR-labeled paramagnetic quantum dots (cNGR-pQDs)³. The cyclic tripeptide ligand cNGR was shown to home specifically to the transmembrane protein CD13, which is upregulated on endothelial cells of angiogenic tumor vessels⁴. The model also provides information on whether the CA distributes throughout the entire tumor or not. This is important since the highest CA induced changes were always observed in the tumor rim. Although this area is known to have the highest level of angiogenic activity, the strong effects in the rim may also be related to the high interstitial pressures in the tumor, thereby preventing CA-delivery in the deeper tumor tissue.

Methods

Contrast agent. Streptavidin coated Cadmium/Selenium quantum dots (585 nm emission) were purchased from Invitrogen. cNGR-pQDs were prepared by mixing QDs, biotin-cNGR ligand and biotin-Gd-DTPA-wedge (containing 8 Gd-DTPA moieties per molecule) in a molar ratio of 1:6:24, as described previously³. Unlabeled (no ligand) particles were prepared similarly. The contrast agent's ionic T_1 relaxivity was $\sim 7 \text{ mM}^{-1}\text{s}^{-1}$ at 7 T.

In vivo MRI. Male athymic Swiss mice received a subcutaneous injection of $\sim 1.5 \times 10^6$ human colon carcinoma cells (LS174T) in the flank. Tumors grew for approximately 14 days and had a size of $\sim 1.0 \text{ cm}^3$ at the day of MRI. Experiments were performed on a 7 T Bruker Biospec 70/30 USR. Seven mice were included for each contrast agent group. Dynamic multi-slice FLASH images with a 13 s dynamic scan interval were recorded with TE 2 ms, TR 100 ms, FA 35°, and a 128×128 matrix. In total, 70 dynamic phases were recorded, including 10 pre-contrast phases. The acquired voxel size was $0.31 \times 0.31 \times 1.2 \text{ mm}^3$.

Pharmacokinetic model. Previously, cNGR-pQDs were found to hardly extravasate from tumor vessels³, thereby limiting the number of compartments of the model to two: the endothelial cell layer of the vessel wall and the vessel lumen. A schematic representation of the resulting model is depicted in Figure 1. The measured tissue CA concentration C_T can be described as: $C_T(t) = v_p \cdot C_p(t) + v_w \cdot C_w(t) = v_p \cdot C_p(t) + C_p(t) \otimes H(t)$. Here, v_p , v_w , C_p and C_w are the fractional plasma volume, the fractional vessel wall volume, the plasma CA concentration, and the concentration of CA bound to the vessel wall, respectively. The tissue transfer function $H(t)$ is given by: $H(t) = K \cdot e^{-\kappa t}$, with the association and dissociation constants K and κ as illustrated in Figure 1. The measured tissue CA concentration C_T can be described as: $C_T(t) = v_p \cdot C_p(t) + v_w \cdot C_w(t) = v_p \cdot C_p(t) + C_p(t) \otimes H(t)$. Here, v_p , v_w , C_p and C_w are the fractional plasma volume, the fractional vessel wall volume, the plasma CA concentration, and the concentration of CA bound to the vessel wall, respectively. The tissue transfer function $H(t)$ is given by: $H(t) = K \cdot e^{-\kappa t}$, with the association and dissociation constants K and κ as illustrated in Figure 1, and $v_w = K/\kappa$. Dynamic changes in signal intensity were assumed to be linearly related to changes in CA concentration. Differences in relaxivity between freely diffusing and bound CA particles were ignored in this approximation. The plasma signal $C_p(t)$ was obtained by measuring the signal changes in a large vessel and multiplying this by (1-Hct), with a hematocrit Hct of 0.45. Subsequent fitting of the tissue time curve $C_T(t)$ by numerical optimization in Matlab provided the pharmacokinetic parameters K , κ and v_p on a voxel-by-voxel basis. Voxels with a fit error greater than 50% were excluded from further analysis. The CA blood half life was determined by fitting $C_p(t)$ to a bi-exponential decay function. All values are presented as mean \pm sem. Statistical analysis was performed using a t-test in SPSS 16.0. $P < 0.05$ was considered significant.

Results

The blood half lives for cNGR- and unlabeled pQDs were 6.5 ± 1.1 and 7.1 ± 1.4 min, respectively ($P = 0.5$), indicating similar systemic behavior. Figure 2 shows axial T_1 -weighted images with color-coded overlay of the parameters K , κ and v_p . cNGR-pQDs displayed higher values for the association parameter K , whereas unlabeled QDs showed higher values for the dissociation parameter κ . The number of voxels with significant increase in K was significantly larger for cNGR- than for unlabeled QDs (11.8 ± 4.7 and $5.7 \pm 1.7\%$, respectively in the highly angiogenic tumor rim, $P = 0.03$). For κ , the percentage of increased voxels was largest for unlabeled pQDs (4.3 ± 2.0 and $7.3 \pm 5.7\%$ for cNGR- and unlabeled pQDs, respectively in the rim, $P = 0.16$). The fractional plasma volume, v_p , was also largest for unlabeled pQDs, although the differences were not significant. Tumor rim and core differences were only significant for the percentage of enhanced voxels on K and v_p when using cNGR-pQDs. Figure 3 shows the percentage of voxels with a significant increase in K versus the distance from the tumor rim. Both CAs showed significant changes in the tumor rim (distance $< 1 \text{ mm}$) as well as in the tumor core (Figures 2 and 3), indicating that the CA-delivery occurs throughout the entire tumor.

Conclusions

The simple two-compartment model provides unique information on the pharmacokinetic behavior of cNGR-pQDs targeted to the angiogenic tumor vasculature, and of non-targeted control particles. A disadvantage of the model is that absolute CA concentrations cannot be determined since the *in vivo* relaxivities are unknown and likely differ for bound and unbound CA. However, as significant changes in all three parameters K , κ and v_p could be detected in the tumor core, this provides evidence that the CAs do perfuse the core and that the differences between tumor rim and core can indeed be ascribed to the higher level of angiogenesis in the rim.

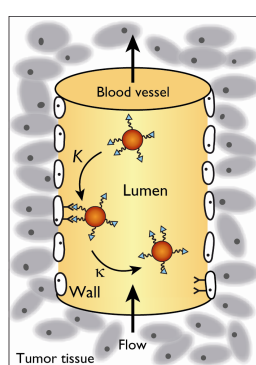


Figure 1. The two compartment model for targeted CAs.

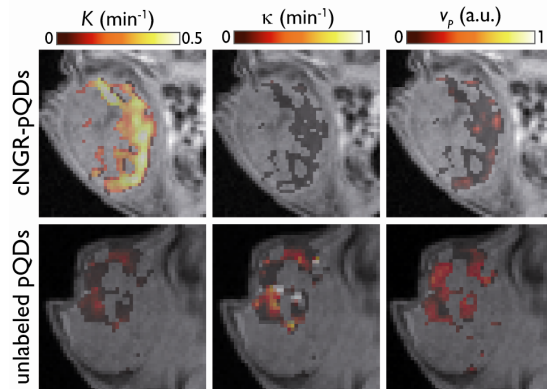


Figure 2. T_1 -weighted anatomical images of the tumors with color-coded K , κ and v_p for cNGR-pQDs and unlabeled pQDs.

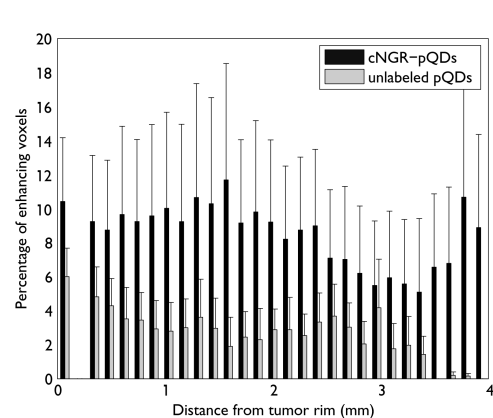


Figure 3. Percentage of voxels with significant enhancement in K versus distance from the tumor rim for cNGR-pQDs (black) and unlabeled pQDs (grey).

References

1. Sipkins DA, et al. *Nat Med* 1998 2. Mulder WJ, et al. *Faseb J* 2005 3. Oostendorp M, et al. *Cancer Res* 2008 4. Pasqualini R, et al. *Cancer Res* 2000
Proc. Intl. Soc. Mag. Reson. Med. 17 (2009) 912